SOLUTE DISPERSION IN AXIALLY STRAINED TUBE FLOWS: LARGE-TIME ASYMPTOTICS AND ORNSTEIN–UHLENBECK GAUSSIAN PROFILES

by Prabakaran Rajamanickam

(*Department of Mathematics and Statistics, University of Strathclyde, Glasgow G1 1XQ, UK*)

[Received 7 June 2025]

Summary

The dispersion of a passive scalar in an axially strained flow in a slender tube is studied, with particular focus on large-time asymptotics following the approach of (**1**). For times exceeding the cross-sectional diffusion timescale, the scalar field forms an axial (Ornstein–Uhlenbeck) Gaussian profile whose variance increases exponentially with the local axial strain, which itself varies with radial location, while radial diffusion only slowly modulates the overall amplitude. In other words, the scalar is dominated by strong axial stretching, completely overwhelming radial diffusion. In striking contrast to classical Taylor dispersion, where radial diffusion rapidly homogenizes the profile and axial convection appears only as a small correction, here axial stretching governs the dominant dynamics, producing a fundamentally different transport mechanism.

1. Introduction

The notion of shear-induced dispersion in laminar pipe flows was first introduced by Taylor (**2**). When a compact distribution of a passive scalar is introduced into a Poiseuille flow, Taylor made two key observations: (1) the center of mass of the scalar cloud is convected downstream with the mean speed, and (2) at times large compared with the radial diffusion time, the scalar distribution becomes radially uniform due to cross-sectional diffusion. At large times, the scalar evolves axially with an enhanced diffusion coefficient arising from the balance between axial stretching (caused by velocity deviations from the mean flow) and radial diffusion. In effect, the Taylor dispersion mechanism corresponds to a homogenization process: the scalar equilibrates over the small scale (tube radius) and manifests as an effective diffusion on the long scale (axial length much greater than the radius). This principle has since been extended to a variety of more complex flow settings including spatio-temporally periodic flows and other generalizations (**3**, **4**, **5**, **6**, **7**, **8**, **9**). A general theory of scalar dispersion in arbitrary laminar flows at large times, however, remains elusive, as the interaction between convection and diffusion can be highly non-trivial.

A particularly important class of flows in fluid mechanics is the family of stagnation-point flows. Dispersion in such flows is fundamentally different from Taylor dispersion. In an early study, Chatwin (1974) (**10**) analysed stagnation-point flows using a Taylor dispersion-like framework, modelling dispersion through an effective diffusion coefficient. More recently, the present author (**1**) demonstrated that this effective-diffusion description is not entirely

accurate, and that the large-time asymptotics must instead be revised to account for the dominance of axial stretching over radial homogenization.

The present paper extends this line of inquiry to the dispersion of a passive scalar in an axially strained tube flow, with particular focus on large-time asymptotics. The objective is twofold: (i) to clearly identify and explain the physical transport mechanism in strained flows, which was only poorly addressed in (**1**), and (ii) to illustrate this mechanism in a canonical tubular geometry, enabling a direct comparison with the classical Taylor-dispersion problem.

Two canonical axially strained flows in tubes are of particular importance: (a) the flow induced by fluid injection through a porous tube, studied by Yuan and Finkelstein (**11**), Taylor (**12**), Culick (**13**) and others, and (b) the flow generated by a linearly stretching tube wall, first analysed by Brady and Acrivos (**14**). For concreteness, this study focuses on the first case, while the second problem appears less trivial and is reserved for future investigation.

2. Problem formulation

Consider the scalar-transport problem in a slender porous tube of circular cross-section with radius a and length $2L$ with $a/L \ll 1$. Fluid is uniformly injected into the tube with a speed V. Both ends of the tube are assumed open, although the analysis also applies if only one end is open. The characteristic radial velocity scales as $V_r^* \sim V$, while the axial velocity scales as $v_z^* \sim VL/a$. In terms of the non-dimensional variables

$$(r, z) = \frac{1}{a}(r^*, z^*), \qquad (v_r, v_z) = \frac{1}{V}(v_r^*, v_z^*), \qquad p = \frac{p_*}{\rho V^2}, \tag{2.1}$$

the self-similar solution is given by

$$v_r = -\frac{2}{r}f(\eta), \qquad v_z = 4zf'(\eta), \qquad p = -\frac{1}{2}(\gamma z)^2 + \Pi(\eta) \tag{2.2}$$

where $\eta = r^2$ and a prime denotes differentiation with respect to η. The function $f'(\eta)$ represents the *local axial strain rate* at different radial locations. Substituting the above ansatz into the axial momentum equation yields the nonlinear eigenvalue problem (**11**)

$$Re^{-1}(\eta f''' + f'') + ff'' - f'^2 = -\tfrac{1}{16}\gamma^2 \tag{2.3}$$

subject to the boundary conditions

$$f(0) = 0, \qquad \lim_{\eta\to 0}\sqrt{\eta}f''(\eta) = 0, \qquad f(1) = \tfrac{1}{2}, \qquad f'(1) = 0. \tag{2.4}$$

Here, $Re = Va/\nu$ is the Reynolds number and the coefficient γ–representing the axial pressure gradient–must be determined as part of the solution. The radial pressure distribution $\Pi(\eta)$ is obtained by integrating the radial momentum equation,

$$\Pi' = \frac{2f^2}{\eta^2} - \frac{4ff'}{\eta} - \frac{4f''}{Re}. \tag{2.5}$$

As $Re \to 0$, the flow approaches a Poiseuille-type flow, whereas as $Re \to \infty$, it tends to the Taylor–Culick flow (**11**, **15**), i.e.,

$$f = \eta - \tfrac{1}{2}\eta^2 + O(Re), \qquad \gamma\sqrt{Re} = 4 + O(Re) \quad \text{as} \quad Re \to 0, \tag{2.6}$$

$$f = \tfrac{1}{2}\sin\frac{\pi\eta}{2} + O(Re^{-1}), \qquad \gamma = \pi + O(Re^{-1}) \quad \text{as} \quad Re \to \infty. \tag{2.7}$$

We now introduce a compact distribution of passive scalar with concentration $c = c_0(r, z)$ in the flow field described above. The equation governing c is given by

$$\frac{\partial c}{\partial t} + Pe\left(v_r\frac{\partial c}{\partial r} + v_z\frac{\partial c}{\partial z}\right) = \frac{1}{r}\frac{\partial}{\partial r}\left(r\frac{\partial c}{\partial r}\right) + \frac{\partial^2 c}{\partial z^2} \tag{2.8}$$

where $t = t^* a^2/D$ is the dimensionless time, $Pe = Va/D = ReSc$ is the Peclet number and $Sc = \nu/D$ is the Schmidt number (or Prandtl number if c represents the temperature field). In terms of η, the governing equation becomes

$$\frac{\partial c}{\partial t} + 4Pe\left(-f\frac{\partial c}{\partial \eta} + zf'\frac{\partial c}{\partial z}\right) = 4\frac{\partial}{\partial \eta}\left(\eta\frac{\partial c}{\partial \eta}\right) + \frac{\partial^2 c}{\partial z^2}. \tag{2.9}$$

We solve this equation in the spatial domain $[0, 1]\times(-\infty, +\infty)$ using the following boundary conditions

$$t = 0: \quad c = g(\eta)\delta(z - z_0), \tag{2.10}$$

$$t > 0: \quad c \to 0 \quad \text{as} \quad |z| \to \infty, \quad \text{and} \quad \sqrt{\eta}\frac{\partial c}{\partial \eta} = 0 \quad \text{at} \quad \eta = 0, 1. \tag{2.11}$$

The initial condition for c corresponds to the release of scalar at a given axial location. The porous surface at $\eta = 1$ is assumed to be impermeable to the scalar. Finally, conservation of the scalar is expressed through the normalization condition

$$\pi\int_0^\infty\int_0^1 c(\eta, z, t)d\eta dz = 1. \tag{2.12}$$

3. Large time asymptotics

We now investigate the solution behaviour for $t \gg 1$ with $Pe \sim 1$, i.e., for time scales much longer than the radial diffusion time a^2/D. One would expect radial diffusion to homogenise the profile at these times, as is the case in the Taylor-dispersion process. However, the axial convection term $4Pezf'$, being proportional to z, is so rapid that the distortion induced by this advection cannot be balanced by radial diffusion. As shown in (**1**), the axial transport of $c = C(z, t; \eta)$ is instead governed by an equation of the form

$$\frac{\partial C}{\partial t} + 4Pezf'\frac{\partial C}{\partial z} = \frac{\partial^2 C}{\partial z^2}. \tag{3.1}$$

Note that η-dependence of C is parametric as it arises only due to the varying axial strain rate $f'(\eta)$. Suppose $C = \delta(z - z_0)$ at $t = 0$. Then the solution to the above equation takes the form

$$C = \frac{1}{\sqrt{2\pi}\sigma}\exp\left[-\frac{(z_0 - ze^{-4Pef't})^2}{2\sigma^2}\right], \qquad \sigma^2 = \frac{1 - e^{-8Pef't}}{4Pef'}, \tag{3.2}$$

which is an Ornstein–Uhlenbeck Gaussian profile. As $t \gg 1$, this approximates (apart from constant factors) to

$$C \approx \exp\left(\frac{-2Pef'z^2}{e^{8Pef't}}\right) \quad \text{if} \quad C_0 \text{ is concentrated at } z = 0, \tag{3.3}$$

$$C \approx \exp\left(\frac{-2Pef'(z - z_0e^{4Pef't})^2}{e^{8Pef't}}\right) \quad \text{if} \quad C_0 \text{ is concentrated at } z = z_0. \tag{3.4}$$

In both cases, the Gaussian structure is still preserved.

The actual large-time solution of c is not just C, but it is modulated by the radial convection and diffusion terms, which have been neglected so far. Following (**1**), we introduce the ansatz

$$c(\eta, z, t) = A(\eta, t)C(z, t; \eta) \tag{3.5}$$

where C is given by (3.4). Introducing this into the full governing equation (2.9) and neglecting higher-order errors in time, we obtain the equation

$$\frac{\partial A}{\partial t} - 4Pef\frac{\partial A}{\partial \eta} = 4\frac{\partial}{\partial \eta}\left(\eta\frac{\partial A}{\partial \eta}\right) \tag{3.6}$$

which is subject to the conditions

$$t = 0: \quad A = g(\eta), \qquad \text{and} \qquad t > 0: \qquad \sqrt{\eta}\frac{\partial A}{\partial \eta} = 0 \quad \text{at} \quad \eta = 0, 1. \tag{3.7}$$

Since we are only interested in the large-time solution, where the initial profile $g(\eta)$ becomes irrelevant, it is sufficient to seek solutions of the form $A = F(\eta)e^{-4\lambda t}$ such that

$$(\eta F')' + PefF' + \lambda F = 0, \qquad \sqrt{\eta}F' = 0 \quad \text{at} \quad \eta = 0, 1. \tag{3.8}$$

This is a Sturm–Liouville problem, possessing positive eigenvalues. The smallest eigenvalue dictates the large-time behaviour. Calculated values of the smallest eigenvalue for the two limiting cases (2.6)-(2.7) are shown in Fig. 1. The corresponding eigenfunction $F(\eta)$ varies monotonically within the interval $[0, 1]$. For small and large values of Pe, we find

$$Pe \to 0: \quad F = J_0(2\sqrt{\lambda\eta}), \qquad \lambda = \tfrac{1}{4}j_{1,1}^2 = 3.6705, \tag{3.9}$$

$$Pe \to \infty: \quad F = \exp(-Pef'(0)\eta), \qquad \lambda = Pef'(0); \tag{3.10}$$

see Appendix for the description of the solution for the second case.

Thus, large-time asymptotic behaviour is given by

$$c = NF(\eta)\exp\left[-4\lambda t - \frac{2Pef'(z - z_0e^{4Pef't})^2}{e^{8Pef't}}\right] \tag{3.11}$$

where N is the normalisation factor. Imposing the conservation of matter condition (2.12)

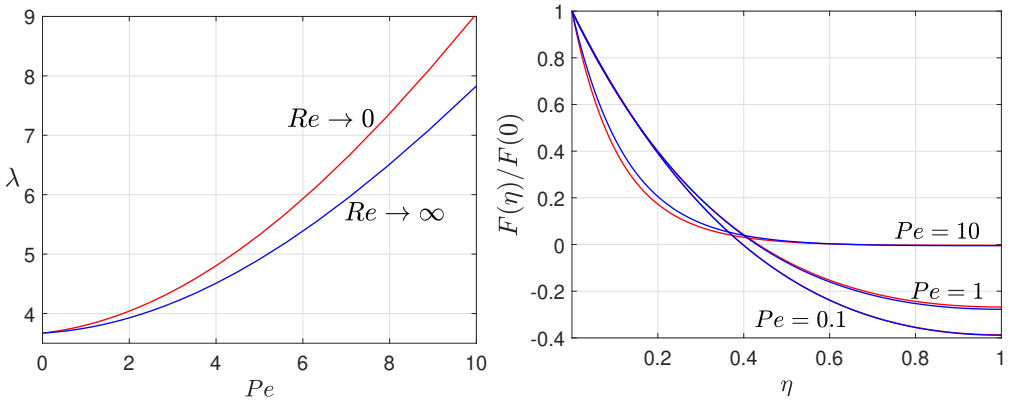

Fig. 1 Left: Smallest eigenvalue of the Sturm–Liouville problem (3.8). Right: Eigenfunctions corresponding to the smallest eigenvalue for three values of Pe. In both plots, red lines correspond to Poiseuille-flow profile (2.6) and the blue lines to the Taylor–Culick profile (2.7).

to determine N, we find

$$N = \frac{e^{4\lambda t}}{\pi}\left[\int_0^1 F(\eta)\sqrt{\frac{\pi}{2Pef'}}e^{4Pef't}d\eta\right]^{-1}, \tag{3.12}$$

$$= \frac{e^{4\lambda t}}{\pi}\left[F(\eta_*)\sqrt{\frac{\pi}{2Pef'(\eta_*)}}e^{4Pef'(\eta_*)t}\sqrt{\frac{2\pi}{4Pe|f'''(\eta_*)|t}}\right]^{-1}, \tag{3.13}$$

$$= \frac{2Pe}{\pi^2 F(\eta_*)}\sqrt{f'(\eta_*)|f'''(\eta_*)|t}e^{4(\lambda - Pef'(\eta_*))t} \tag{3.14}$$

where in the second step, the integral is approximated using Laplace's method, where η_* denotes the location at which $f'(\eta)$ reaches its maximum. Thus, putting everything together, we finally obtain

$$c = \frac{2Pe}{\pi^2}\sqrt{f'(\eta_*)|f'''(\eta_*)|t}\frac{F(\eta)}{F(\eta_*)}\exp\left[-4Pef'(\eta_*)t - \frac{2Pef'(z - z_0e^{4Pef't})^2}{e^{8Pef't}}\right] \tag{3.15}$$

For our problem, $\eta_* = 0$; furthermore as $Re \to 0$, $f''' \sim O(Re)$, whereas as $Re \to \infty$, $f'''(0) = -\pi^3/16$. It is interesting to note that the eigenvalue λ disappears since the normalization condition forces the solution to adjust so that only the shape of the eigenfunction $F(\eta)$ matters, not its eigenvalue. The actual decay in time, is determined by the factor $f'(\eta_*)t$ and not by λt. In (**1**), the opposite conclusion was made erroneously.

4. Concluding remarks

This study has examined the dispersion of a passive scalar in an axially strained flow within a slender tube, focusing on the large-time asymptotic behaviour. Unlike classical Taylor dispersion, where radial diffusion rapidly homogenizes the scalar across the tube and axial advection only appears as a perturbation, the present analysis demonstrates that axial

stretching dominates the scalar evolution. As a result, the scalar forms an Ornstein—Uhlenbeck Gaussian profile along the axis whose variance grows exponentially with the local axial strain $f'(\eta)t$, while radial diffusion merely provides a slow modulation of the amplitude. The overall concentration decay rate is determined by the maximum axial strain $f'(\eta_*)t$ where axial stretching is dominant.

The study highlights a fundamentally different mechanism of dispersion in pipe flows: axial convection, rather than radial diffusion, controls the scalar transport when the observation time is large compared with the radial diffusion timescale. The analysis provides explicit expressions for the evolving scalar field, including its normalization, and shows how the classical assumption of an effective axial diffusion coefficient breaks down in this setting. Particularly, it is meaningless to talk about the cross-sectionally averaged concentration, since deviations from the mean value are not small.

Overall, the results clarify the physics of scalar transport in axially strained flows and provide a quantitative framework for predicting the rate and structure of large-time dispersion. This offers a clear contrast with traditional Taylor dispersion and suggesting potential strategies for targeted solute transport in practical applications.

It would be interesting to extend the study in the future to the flow field considered by Brady and Acrivos (**14**), where the local strain rate undergoes a reversal of sign ($f'(\eta) < 0$) within the tube. In such cases, the scalar cloud may be compressed rather than stretched, potentially leading to steep axial gradients. Regions with $f' < 0$ may act as local temporary traps, delaying its transport until radial diffusion eventually spreads it out. Nevertheless, the maximal positive $f'(\eta)$ is likely to control the leading-order large-time transport, although a more detailed analysis is required. Other interesting directions for future study include axially strained flows with complex Burgers'-type vortex structures (**16**, **17**, **18**).

Appendix: Eigenvalue calculation for large Peclet numbers

The solution to the eigenvalue problem (3.8) is given here. Taking the limit $Pe \to \infty$, we obtain

$$Pef F' + \lambda F = 0, \quad \Rightarrow \quad F = C \exp\left(\frac{\lambda}{Pe}\int_\eta^1 \frac{d\hat{\eta}}{f(\hat{\eta})}\right) \tag{4.1}$$

To satisfy the boundary condition at $\eta = 1$, we must set $C = 0$. Thus, $F = 0$ in the outer region, and a thin boundary layer prevails near $\eta = 0$ with thickness $\eta \sim 1/Pe$. Introducing the stretched variables

$$\xi = Pe\,\eta, \qquad \Lambda = \frac{\lambda}{Pe} \tag{4.2}$$

the leading-order equation becomes

$$\frac{d}{d\xi}\left(\xi\frac{dF}{d\xi}\right) + f'_*\xi\frac{dF}{d\xi} + \Lambda F = 0 \tag{4.3}$$

where $f'_* = f'(0)$. This must be supplemented with

$$\lim_{\xi\to 0}\sqrt{\xi}\frac{dF}{d\xi} = 0 \quad \text{and} \quad F(\infty) \to 0\,(\text{exponentially}). \tag{4.4}$$

The solution that obeys the condition at the origin is given by

$$F \sim e^{-f'_*\xi} M\left(1 - \frac{\Lambda}{f'_*}, 1, f'_*\xi\right) \tag{4.5}$$

where M is the confluent hypergeometric function. Its asymptotic expansion as $\xi \to \infty$ consists of an algebraically decaying component,

$$F \sim (f'_*\xi)^{-\Lambda/f'_*}/\Gamma(1-\Lambda/f'_*) \tag{4.6}$$

and an exponentially decaying component

$$F \sim e^{-f'_*\xi}(f'_*\xi)^{\Lambda/f'_*-1}/\Gamma(\Lambda/f'_*). \tag{4.7}$$

To eliminate the algebraically decaying part and retain only exponential decay, the prefactor mush vanish. This occurs when

$$\frac{1}{\Gamma(1-\Lambda/f'_*)} = 0, \quad \Rightarrow \quad \Lambda_n = f'_*(1+n), \qquad n = 0, 1, 2, 3, \ldots \tag{4.8}$$

so that the eigenfunctions reduce to

$$F_n = e^{-f'_*\xi}L_n(f'_*\xi) \tag{4.9}$$

where L_n is the Laguerre polynomial. The leading eigenmode corresponds to

$$\Lambda_0 = f'_*, \qquad F_0 = e^{-f'_*\xi}. \tag{4.10}$$

The selection of eigenvalues based on eliminating the algebraically decaying component of the confluent hypergeometric function is essentially similar to the approach studied in (**19**, **20**).

References

1. P. Rajamanickam. Dispersion of solute in straining flows and boundary layers. *Phys. Fluids*, 32(5), 2020.

2. G. I. Taylor. Dispersion of soluble matter in solvent flowing slowly through a tube. *Proc. Roy. Soc. Lond. A. Math. Phys. Sci.*, 219(1137):186–203, 1953.

3. E. J. Watson. Diffusion in oscillatory pipe flow. *J. Fluid Mech.*, 133:233–244, 1983.

4. M. E. Erdogan and P. C. Chatwin. The effects of curvature and buoyancy on the laminar dispersion of solute in a horizontal tube. *J. Fluid Mech.*, 29(3):465–484, 1967.

5. L. B. Prigozhin. Solute dispersion in a pulsating flow. *Fluid Dyn.*, 17(5):674–679, 1982.

6. A. J. Majda and P. R. Kramer. Simplified models for turbulent diffusion: Theory, numerical modelling, and physical phenomena. *Phys. Rep.*, 314(4-5):237–574, 1999.

7. P. Rajamanickam and J. Daou. Effective Lewis number and burning speed for flames propagating in small-scale spatio-temporal periodic flows. *Combust. Flame*, 258:113077, 2023.

8. P. Rajamanickam. Shear-induced force and dispersion due to buoyancy in a horizontal Hele-Shaw cell. *Q. J. Mech. Appl. Math.*, 78(2):hbaf007, 2025.

9. P. Rajamanickam and A. D. Weiss. Taylor dispersion in variable-density, variable-viscosity pulsatile flows. *arXiv preprint arXiv:2503.19623*, 2025.

10. P. C. Chatwin. The dispersion of contaminant released from instantaneous sources in laminar flow near stagnation points. *J. Fluid Mech.*, 66(4):753–766, 1974.

11. S. W. Yuan and A. B. Finkelstein. Laminar pipe flow with injection and suction through a porous wall. *Trans. ASME*, 78(4):719–724, 1956.

12. G. I. Taylor. Fluid flow in regions bounded by porous surfaces. *Proc. Roy. Soc. Lond. A. Math. Phys. Sci.*, 234(1199):456–475, 1956.

13. F. E. C. Culick. Rotational axisymmetric mean flow and damping of acoustic waves in asolid propellant rocket. *AIAA J.l*, 4(8):1462–1464, 1966.

14. J. F Brady and A. Acrivos. Steady flow in a channel or tube with an accelerating surface velocity. an exact solution to the Navier–Stokes equations with reverse flow. *J. Fluid Mech.*, 112:127–150, 1981.

15. S. Balachandar, J. D. Buckmaster, and M. Short. The generation of axial vorticity in solid-propellant rocket-motor flows. *J. Fluid Mech.*, 429:283–305, 2001.

16. A. Liñán, V. N. Kurdyumov, and J. Soler. The flow field in the slender combustion chambers of solid propellant rockets. In F. J. Higuera, J. Jiménez, and J. M. Vega, editors, *Simplicity, Rigor and Relevance in Fluid Mechanics: A Volume in Honor of Amable Liñán*, pages 128–140. CIMNE, 2004.

17. V. N. Kurdyumov. Steady flows in the slender, noncircular, combustion chambers of solid propellant rockets. *AIAA J.*, 44(12):2979–2986, 2006.

18. P. Rajamanickam. Axially strained flow in a porous duct of circular-sector cross-section. *arXiv preprint arXiv:2508.12151*, 2025.

19. A. C. Robinson and P. G. Saffman. Stability and structure of stretched vortices. *Stud. Appl. Math.*, 70(2):163–181, 1984.

20. P. Rajamanickam and A. D. Weiss. Steady axisymmetric vortices in radial stagnation flows. *Q. J. Mech. Appl. Math.*, 74(3):367–378, 2021.